MOLECULAR AND CELLULAR BIOLOGY, Aug. 1987, p. 2845–2856
0270-7306/87/082845-12$02.00/0

Vol. 7, No. 8

# Heterologous Expression and Characterization of the Human R-*ras* Gene Product

DAVID G. LOWE AND DAVID V. GOEDDEL*

*Department of Molecular Biology, Genentech, Inc., South San Francisco, California 94080*

Received 9 March 1987/Accepted 21 May 1987

**We directly expressed human R-*ras* 23,000-dalton protein (p23) cDNA in *Escherichia coli* under the control of the *trp* promoter. GTP-dependent phosphorylation of a p23 threonine 85 substitution mutant was observed. This result is in direct analogy to the autokinase activity of H-*ras* and K-*ras* threonine 59 substitution mutants. Normal p23 protein was detected in the human fibrosarcoma cell line HT1080 by immunoprecipitation with rabbit antibodies raised against an *E. coli*-expressed R-*ras* fusion protein. The R-*ras* p23 protein was found to be $^3$H labeled in the presence of [9,10(*n*)-$^3$H]palmitic acid and is associated with the P100 membrane fraction of HT1080 cells. These data suggest that human R-*ras* p23 has biochemical properties very similar to those of the p21 products of the H-, K-, and N-*ras* proto-oncogenes. We constructed an R-*ras* minigene and engineered the expression of normal and mutant alleles from the simian virus 40 early region promoter. Normal and mutant R-*ras* gene products were authenticated by transient expression in COS-7 cells and immunoprecipitation. The valine 38-substituted R-*ras* p23 displayed reduced electrophoretic mobility. R-*ras* p21-like proteins, made by eliminating the first 26 R-*ras* codons, displayed evident mobility differences between the pro form and mature form, along with a valine 12 substitution-dependent change in electrophoretic mobility. Rat-1 fibroblasts were transfected with normal and mutant R-*ras* alleles and normal and activated H-*ras* alleles. Unlike the human T24 bladder oncogene-encoded p21, mutant R-*ras* alleles do not cause monolayer focus formation or growth in soft agar of rat fibroblasts.**

The human genome contains three closely related proto-oncogenes, H-*ras1*, K-*ras2*, and N-*ras*, which encode closely related 21,000-dalton proteins (p21s) of 188 to 189 amino acids (5, 6, 38, 57, 64). These genes were first identified through their mutant alleles, found as the transforming genes in transducing retroviruses and in high-molecular-weight tumor DNA (67). To understand the dominant phenotype of mutant *ras* genes in malignant transformation, considerable attention has been paid to the biochemical properties of *ras* p21 proteins (70). H-*ras* p21 is synthesized on free ribosomes as pro-21 (56), whereupon it is modified to its mature form by the addition of palmitic acid to cysteine 186 (8, 72, 73) and is localized to the inner surface of the plasma membrane (71). The H-, K-, and N-*ras* p21s are GTP-binding proteins with intrinsic GTPase activity (17, 37, 51, 62). The unique regulatory roles of GTP-binding proteins (27) and the biochemical similarities between *ras* p21s and the adenylyl cyclase G proteins (18, 27) suggest that *ras* proteins play a role in cell surface signal transduction.

By virtue of nucleic acid sequence homology to viral H-*ras*, we recently cloned another member of the mammalian *ras* gene family, R-*ras* (33). The predicted human R-*ras* gene product of 218 amino acids and 23,400 daltons (p23) has an amino-terminal extension of 26 amino acids relative to the H-, K-, and N-*ras* p21s. The predicted amino acid sequence of R-*ras* p23 is 55% identical in the region of overlap with H-*ras* p21, with invariantly conserved regions including the predicted guanine-nucleotide binding site and the palmitation sequence Cys-A-A-X, where A is an aliphatic amino acid and X is the carboxyl-terminal amino acid (33). Based on the known characteristics of the H-, K-, and N-*ras* p21 molecules and the predicted sequence similarity of p21 proteins and R-*ras* p23, we characterized some biochemical properties of R-*ras* p23. Our studies of R-*ras* p23 suggest that, like *ras* p21s, the protein is a membrane-localized GTPase that may be involved in membrane signal transduction. To investigate the relative properties of R-*ras* p23 and *ras* p21 proteins, we chose in vitro rat fibroblast transformation as a comparative assay for the biological activity of mutant R-*ras* p23 alleles and activated H-*ras* p21. In contrast to the activated H-*ras* gene, analogous R-*ras* mutants do not contribute to focus formation or soft-agar growth by rat fibroblasts. Our results indicate that, although biochemically similar, *ras* p21 proteins and R-*ras* p23 may have different biological functions.

## MATERIALS AND METHODS

**Expression plasmid construction and mutagenesis.** The *Escherichia coli* direct expression vector pBTE4 (R. Derynck, unpublished data) was digested with *Xba*I and *Eco*RI, and the 4.3-kilobase vector fragment was purified by polyacrylamide gel electrophoresis (PAGE) and electroelution. Synthetic DNA fragments were designed to replace the first 21 codons of the R-*ras* amino-terminal coding sequence: (i) 5′-CTAGAATTATGAGCTCTGGTGCTGCTTCTG (with the *Xba*I half-site and the initiator methionine codon underlined), (ii) 5′-GTACAGGTCGTGGTCGTCCACGTGGTGG AGGTCCAGGTCCC (ending at the *Sma*I half-site of codon 21), and the partially complementary oligonucleotides (iii) 5′-GGGACCTGGACCTCCACCACGTGGACGACCACG and (iv) 5′-ACCTGTACCAGAAGCAGCACCAGAGCTC ATAATT. The last three oligonucleotides named were 5′-phosphorylated using T4 polynucleotide kinase prior to annealing of all four oligonucleotides and ligation to the 890-base-pair (bp) *Sma*I-*Eco*RI fragment from R-*ras* cDNA clone HR-1.1 (33). The DNA was digested with *Eco*RI, 5′-phosphorylated with T4 polynucleotide kinase, and electrophoresed through a 6% polyacrylamide gel, and the 961 bp *Xba*-*Eco*RI fragment was purified by electroelution. The purified DNA fragment was ligated to the pBTE4 *Xba*I-

* Corresponding author.

*Eco*RI fragment, and the resulting recombinant plasmid pTRGA was used to transform *E. coli* K-12 strain 294 (1) to ampicillin resistance.

To verify the structure of pTRGA, the 961-bp *Xba*I-*Eco*RI linker-cDNA fragment was isolated and cloned into M13 mp19 (76) for dideoxynucleotide sequencing (49). Using M13 mp19–R-*ras* (*Xba*I-*Eco*RI) as a template, we followed the double-primer strategy of Zoller and Smith (77) to mutate R-*ras* codon 85 Ala (GCG) to Thr (ACC) with the oligonucleotide 5′-TTCCTGGCCGGTGGTGTCCAG (the mutant anticodon is underlined) and a protection primer, 5′-TTGCCCACCTCGTTGAAA, which hybridizes 80 nucleotides 5′ of the mutagenesis primer. To identify mutants, $^{32}$P-labeled mutagenesis primer was hybridized to M13 plaques on nitrocellulose (77) and filters were washed at room temperature in 0.15 M NaCl–0.015 sodium citrate (1× SSC)–0.1% sodium dodecyl sulfate (SDS) for 15 min before autoradiography. Positively hybridizing plaques were picked for subsequent DNA sequence analysis (49). The vector pTRGT, for expression of R-*ras* with the position 85 mutation Ala → Thr, was constructed by preparing a double-stranded fragment of the mutant R-*ras* cDNA sequence from M13 mp19 (*Xba*I-*Eco*RI) and cloning it into the pBTE4 *Xba*I-*Eco*RI vector fragment.

For construction of the R-*ras* fusion protein expression vector pLER, oligonucleotides i and iv (see above) were replaced with the oligonucleotides (v) 5′-AATTCATG AGCTCTGGTGCTGCTTCTG (the R-*ras* first methionine codon is underlined) and (vi) 5′-ACCTGTACCAGAAG CAGCACCAGACTCATG to give an *Eco*RI-cohesive 5′ end. The R-*ras* *Eco*RI-*Eco*RI linker-cDNA fragment was constructed as described above for the *Xba*I-*Eco*RI fragment and linked via the *Eco*RI site to the in-frame coding sequence of the *trpLE* medium fusion plasmid pMNCV (Derynck, unpublished data), in which sequences from codon 16 to 188 (20) and 219 to 307 have been deleted from the Δ*trp LE1413* fusion (39). The resulting 101-amino-acid *trp* medium-fusion sequence is devoid of cysteine residues. *E. coli* K-12 strain 294 (1) was transformed to tetracycline resistance, and pLER plasmid clones were identified by restriction mapping to determine the correct orientation of the linker–R-*ras* *Eco*RI fragment.

For mammalian expression vector contruction, the 5.17-kilobase *Eco*RI fragment containing the six coding exons of the human R-*ras* gene (33) was cloned into the *Eco*RI site of pUC12 (pUC plasmid with M13 mp10 polylinker) (44). A plasmid clone, pUCR, was chosen in which the remaining vector polylinker cloning sites were arranged at the 3′ end of the R-*ras* *Eco*RI fragment. The first four coding exons of the R-*ras* gene in pUCR were replaced with R-*ras* cDNA sequences from the *Apa*I site 62 bp 3′ of the initiator methionine codon to the *Bgl*II site 21 bp 5′ of the exon 4 splice donor site (33). The 4.5-kilobase *Apa*I-*Bgl*II pUCR vector fragment containing R-*ras* genomic sequences flanking the cDNA substitution was purified by electroelution from a polyacrylamide gel and ligated to gel-purified 149-bp *Apa*I-*Pst*I and 220-bp *Pst*I-*Bgl*II R-*ras* cDNA fragments, which encompass the exon 1 to exon 4 cDNA substitution. The resulting three-exon minigene plasmid was designated pUCRM. To confirm the structure of the first R-*ras* minigene exon and to create a template for in vitro mutagenesis of R-*ras* codons 27 and 38, the 854-bp *Eco*RI-*Sph*I pUCRM exon 1 fragment was cloned into M13 mp18 (76) for dideoxynucleotide sequencing (49). Mutagenesis of R-*ras* codon 38 Gly (GGC) to Val (GTC) was achieved with the mutant oligonucleotide 5′-CCCACGCCGACGCCGCCCA and a protection primer, 5′-TTGCCCACCTCGTTGAAA, which hybridizes 222 bp 5′ of the mutagenesis primer. R-*ras* codon 27 Ser (AGC) was mutated to Met (ATG) by using the mutant oligonucleotide 5′-GTGTGTCTCCATGGGCGGGG and the protection primer 5′-GGGATGCCATCCACA CTG, which hybridizes 119 bp 5′ of the mutagenesis primer. The R-*ras* expression vectors utilizing the SV40 early promoter consisted of the *Bam*HI-*Eco*RI vector fragment of pML-1 (34) with the *Eco*RI site fused to the *Hin*cII site of the *Hin*cII-*Hin*dIII 600-bp fragment of SV40 (13) that contains the 72-bp repeats and early promoter. A synthetic oligonucleotide, 5′-AGCTTATCGATTCTAGAATTC, was fused to the *Hin*dIII site to provide the polylinker sequence *Hin*dIII, *Cla*I, *Xba*I, *Eco*RI (A. D. Levinson, unpublished data). The pML-1 *Bam*HI site was linked to the *Bgl*II site of the 585-bp *Bam*HI-*Bgl*II fragment of the hepatitis B surface antigen gene 3′ untranslated region (10). The *Eco*RI-*Bam*HI promoter/terminator-vector fragment was used to construct R-*ras* expression plasmids pSVE.RG (Gly 38) and pSVE.RV (Val 38 mutant allele) with the *Eco*RI-*Sph*I exon 1 fragment from pUCRM (for pSVE.RG), or from filled-in M13 mp19 *Eco*RI-*Sph*I Gly 38 → Val mutant (for pSVE.RV), plus the *Sph*I-*Bam*HI 3′ gene fragment for pUCRM (utilizing the pUC12 *Bam*HI polylinker site). The R-*ras* amino-terminal deletion plasmids pSVE.RGΔ1-26 and pSVE.RVΔ1-26 were constructed using the *Sma*I site spanning R-*ras* codons 21 and 22 to ligate to the *Eco*RI site at the 3′ end of the SV40 promoter, which was filled in using DNA polymerase I (Klenow fragment) and deoxynucleoside triphosphates. The use of this *Sma*I site in the R-*ras* coding sequence removed the first methionine codon and allowed the use of the codon 27 Ser → Met mutant (see above) to provide a new start site for translation.

For cotransformation and selection, the plasmid pNeo DHFR was constructed using the *Bam*HI-*Sal*I fragment of pMTE4E (48), which contains, in order of 5′ to 3′, an SV40 early promoter linked to the aminoglycosyl phosphotransferase II gene (59), followed by the hepatitis B surface antigen gene 3′ untranslated region (10) and an SV40 early promoter linked to dihydrofolate reductase coding sequence (58) and the hepatitis B surface antigen gene 3′ untranslated region. This pMTE4E *Bam*HI-*Sal*I fragment was cloned into the *Bam*HI-*Sal*I vector fragment of pML-1 (34) to give pNeoDHFR.

**Bacterial growth and induction of R-*ras*.** *E. coli* K-12 strain 294 (1) was either transformed to ampicillin resistance with pTRGA, pTRGT, or pBR322 or transformed to tetracycline resistance with pLER or pBR322. Colonies of freshly transformed *E. coli* were inoculated into L-broth liquid cultures plus either ampicillin or tetracycline at 5 μg/ml and grown at 37°C to an $A_{550}$ of 0.2 to 0.5. Cultures were chilled on ice, and appropriate amounts were centrifuged at 3,000 × *g* for 5 min and suspended in M9 medium minus $CaCl_2$ at a final $A_{550}$ of 0.2. Cultures were incubated for 20 to 30 min at 37°C, and R-*ras* expression was then induced by adding to the cultures indoleacetic acid (IAA) to 20 μg/ml. Cultures were further incubated at 37°C to a final $A_{550}$ of 0.9 to 1.0 for R-*ras* direct expression, or to 0.4 to 0.8 for R-*ras* fusion protein expression. Bacteria were collected by centrifugation, and whole-cell extracts were prepared for SDS-PAGE (29) as described by Derynck et al. (12). SDS-PAGE fractionated proteins were stained with Coomassie brilliant blue.

**In vitro kinase assay.** A Triton X-100 lysate of *E. coli* cells was prepared by a modification of the procedure of Clark et al. (9). Cells from 20-ml cultures were suspended in 600 μl of 50 mM glucose–25 mM Tris hydrochloride (pH 8.0)–10 mM

EDTA–5 mg of lysozyme per ml–0.01% aprotinin–1 mM phenylmethylsulfonyl fluoride and incubated at 4°C for 30 min. Then, 20% Triton X-100 was added to 1% (vol/vol), and the solution was further incubated at 4°C for 5 min. Cellular debris was removed by centrifugation at 18,000 × *g* for 10 min at 4°C. The supernatant was treated with 0.5% polyethyleneimine (pH 8.0) for 10 min at 4°C and then centrifuged at 18,000 × *g* for 5 min. A 100-μl portion of this cell extract was adjusted to 5 mM $MgCl_2$–100 mM NaCl–2 mM dithiothreitol–1 mM rATP–33 μM [$\gamma$-$^{32}$P]GTP (Amersham, 30 Ci/mmol) and incubated at 37°C for 60 min.

**R-*ras* antibody production.** A synthetic oligopeptide beginning with an amino-terminal cysteine residue followed by the R-*ras* sequence 191-209 (Arg-Lys-Tyr-Gln-Glu-Gln-Glu-Leu-Pro-Pro-Ser-Pro-Pro-Ser-Ala-Pro-Arg-Lys-Lys) (33) was conjugated to soybean trypsin inhibitor with the sulfhydryl reagent maleimidobenzoyl sulfosuccinimide ester (Sulfo-MBS; Pierce). Two New Zealand white rabbits were each immunized with 200 μg of peptide-soybean trypsin inhibitor conjugate in 3 volumes of Freund complete adjuvant by multiple-site intradermal injection. At 2-week intervals the rabbits were then boosted with 50 μg of peptide-soybean trypsin inhibitor conjugate in 3 volumes of Freund incomplete adjuvant by multisite subcutaneous injection. Ten days after the second boost, the animals were test bled, and after the third boost the recovery period between injections was increased to 4 weeks, with test bleeds 10 to 14 days postboost. To provide an antigen to test for the production of R-*ras* oligopeptide antibodies by immunoblotting (see below), the oligopeptide was coupled to bovine serum albumin (fraction V; Sigma) by using the lysine reagent bis(sulfosuccinimidyl) suberate (Pierce).

To produce antisera against the LE–R-*ras* medium fusion protein, rabbits were immunized with polyacrylamide gel slices containing LE–R-*ras* protein (4). Antigen was prepared by SDS-PAGE fractionation of the *E. coli* whole-cell lysate (see above), using a single-slot gel comb. The appropriate region of the gel was excised, chopped with a razor blade, and then homogenized in an equal volume of Freund incomplete adjuvant by successively forcing through 18, 20, and 22 gauge needles broken to 0.5 cm in length. Each of two New Zealand white rabbits was inoculated with the LE–R-*ras* protein, derived from a 20-ml culture grown to $A_{550}$ of 0.75 to 0.80, by multiple-site subcutaneous injections. Rabbits were boosted and test bled by the schedule described above, and antibody production was assayed by probing immunoblots (see below) of R-*ras* directly expressed in *E. coli*.

**Immunoblotting and immunoprecipitation of *E. coli*-expressed R-*ras*.** Protein samples were fractionated by SDS-PAGE in 0.75-mm-thick gels and electrophoretically transferred to nitrocellulose (BA85, 0.45-μm pore size; Schleicher and Schuell) in 25 mM Tris hydrochloride–192 mM glycine (pH 8.3) (65). The nitrocellulose filter was allowed to air dry for 30 min after transfer, blocked by incubating for 30 min at room temperature in 3% Norland gelatin in phosphate-buffered saline (PBS) (50), and then rinsed in PBS plus 0.05% polyoxyethylene sorbitan monolaurate (Tween 20; Sigma) for 10 min (Bio-Rad Immun-Blot Instruction Manual). Antibody binding was in PBS–1% gelatin, plus rabbit serum diluted 1:100, for 2 h. Filters were rinsed for 10 s in $H_2O$ and twice in PBS–0.05% Tween 20 for 10 min each. Goat anti-rabbit horseradish peroxidase conjugate (Cappel Laboratories) was incubated with the filter at a 1:1,000 dilution in PBS–0.05% Tween 20 for 2 h. The filter was washed as described above plus an additional 10-min wash in PBS. The color reaction was initiated by mixing 60 mg of 4-chloro-1-napthol (Bio-Rad) in 20 ml of methanol with 60 μl of $H_2O_2$ in 100 ml of PBS and stopped by rinsing the filter in PBS.

For immunoprecipitation of R-*ras* from *E. coli* Triton X-100 lysates (see above), extracts were adjusted to 0.5% sodium deoxycholate–0.5% Nonidet P-40–0.1% SDS–0.1% bovine serum albumin in PBS by the addition of a two-times-concentrated detergent solution and were pretreated with 20 μl of a 50% (wt/vol) protein A-Sepharose (PAS) solution for 15 min at 4°C. The PAS was removed by centrifugation, and the pretreated *E. coli* extract was incubated with antipeptide serum at a 1:100 dilution for 60 min at 4°C. Antigen-antibody complexes were absorbed to 20 μl of 50% (wt/vol) PAS for 10 min at 4°C. The PAS was pelleted by centrifugation and washed four times in 50 mM Tris (pH 8.0)–0.5% Nonidet P-40–0.12 M NaCl–1 M LiCl (9). Proteins were eluted from the PAS by boiling in sample mix (29), fractionated by SDS-PAGE, and either blotted to nitrocellulose (see above) or impregnated with En$^3$Hance (New England Nuclear Corp.) before fluorography.

**Metabolic labeling of HT1080 cells and immunoprecipitation.** The human fibrosarcoma cell line HT1080 (American Type Culture Collection CCL121) was labeled in minimum essential medium (MEM) minus cysteine and methionine (GIBCO, Selectamine), plus 160 μCi each of L-[$^{35}$S] cysteine and L-[$^{35}$S]methionine (Amersham) per ml, for 4 h. Labeling of HT1080 cells with [9,10(*n*)-$^3$H]palmitic acid (Amersham) at 250 μCi/ml was in Dulbecco MEM plus 5% dialyzed calf serum for 16 h. Immunoprecipitation of R-*ras* p23 from labeled HT1080 cells with fusion-protein antiserum was performed exactly as described by Platt et al. (47). Immunoprecipitation samples were analyzed by SDS-PAGE and fluorography.

**Subcellular fractionation.** Crude membrane and cytoplasmic fractions from labeled HT1080 cells were prepared by a modification of the procedure of Napier et al. (42). Cells were scraped from culture dishes in 1 mM $NaHCO_3$ (pH 7.5)–1 mM phenylmethylsulfonyl fluoride and lysed with 30 strokes of a Dounce homogenizer at 0°C. Nuclei were pelleted by spinning at 2,000 rpm in a Sorvall SS-34 rotor for 15 min at 4°C. The supernatant from this centrifugation was then spun at 100,000 × *g* in a Beckman SW55 Ti rotor for 30 min at 4°C. The supernatant fraction (S100) was adjusted to a final concentration of 1% Triton X-100–0.5% sodium deoxycholate–25 mM Tris hydrochloride (pH 7.5)–250 mM NaCl–5 mM EDTA (lysis buffer) (34). The membrane pellet was suspended in lysis buffer, and insoluble material was removed by centrifugation at 4,000 rpm in a Sorvall HB-4 rotor for 15 min at 4°C. The resulting P100 membrane and S100 cytoplasmic fractions were analyzed by immunoprecipitation (47) with LE–R-*ras* fusion protein antiserum, SDS-PAGE, and fluorography.

**R-*ras* transient expression.** COS-7 cells (19) were grown in high-glucose Dulbecco MEM plus 10% fetal calf serum to approximately 50% confluency in 100-mm culture dishes. Calcium phosphate-DNA coprecipitates were prepared (22) with 20 μg of plasmid DNA, added to the COS-7 cells, and incubated for 5 to 6 h. At the end of the incubation, cells were glycerol shocked (14) with 20% glycerol in PBS for 1 min, rinsed several times in PBS, and incubated in medium for an additional 38 h. Transfected cells were labeled with L-[$^{35}$S]methionine and L-[$^{35}$S]cysteine (Amersham) and analyzed for R-*ras* expression by immunoprecipitation with LE–R-*ras* fusion protein antiserum, SDS-PAGE, and fluorography. To detect posttranslational processing of R-*ras* p23, transfected COS-7 cells were labeled with 66 μCi of

[9,10(*n*)-$^3$H]palmitate (Amersham) per ml in Dulbecco MEM plus 5% dialyzed calf serum from 30 to 46 h posttransfection. R-*ras* proteins were immunoprecipitated with fusion-protein antiserum, and one-half of each of the pansorbin-antibody-antigen pellets from pSVE.RG- and pSVE.RGΔ1-26-transfected cells was treated with 1 M $H_2NOH$-HCl (pH ~ 7.0) (36, 45) at 23°C for 60 min before SDS-PAGE and fluorography. Exposed film was scanned with an LKB 2202 Ultrascan laser densitometer, linked to a Hewlett-Packard 3390A integrator, to detect $^3$H-labeled R-*ras* proteins.

**Cellular transformation assays.** Fischer rat (Rat-1) fibroblasts were maintained in Hams F12 and Dulbecco MEM (50:50) plus 10% fetal calf serum. Samples of $4 \times 10^5$ to $5 \times 10^5$ Rat-1 cells in 60-mm dishes were transfected with 5 μg of plasmid DNA (see above) for monolayer focus assays. At 16 h after glycerol shock, plates were trypsinized and plated onto four or six 100-mm dishes. Monolayer cultures were maintained by feeding every 3 days for 14 to 21 days. Cells were stained with 0.5% (wt/vol) crystal violet (Sigma) in methanol-glacial acetic acid (3:1) and scored for focus formation.

For cotransformation and selection, 5 μg of plasmid DNA was mixed with 0.5 μg of pNeoDHFR for transfection (see above). At 24 h after transfected cells were plated onto 100-mm dishes, the antibiotic geneticin (G418, GIBCO) was added to the medium at 400 μg/ml. Cultures were maintained for 2 weeks in selective medium with fresh medium added every 3 days. At the end of this period, 50 to 100 G418-resistant colonies were trypsinized, pooled, and replated for a monolayer focus assay in nonselective medium, or counted and plated in 2 ml of McCoy 5A (Gibco) medium plus 10% fetal calf serum containing 0.3% Noble agar (Difco) in 12-well dishes. Pooled cultures were plated at densities of $0.25 \times 10^4$, $0.5 \times 10^4$, and $1 \times 10^4$ cells per ml as described (48). Cultures were maintained at 37°C in 5% $CO_2$ for 7 to 14 days, and viable colonies were visualized by staining each well with 1 ml of 0.05% iodonitrotetrazolium (Sigma) overnight at 37°C.

## RESULTS

**Expression of R-*ras* in *E. coli*.** In an effort to obtain sufficient quantities of the R-*ras* p23 protein for biochemical analysis, we adopted the strategy of direct expression of R-*ras* cDNA in *E. coli*. In the absence of a full-length human R-*ras* cDNA clone, and in the presence of a very GC-rich amino-terminal coding sequence (33), we chose to replace the first 21 codons of R-*ras* with a synthetic linker utilizing frequently occurring *E. coli* codons (23). An *Xba*I cohesive terminus was created starting 8 bp 5′ of the R-*ras* translation initiation codon to bring the expression of R-*ras* p23 under the control of the *E. coli trp* promoter and the *trp* ribosome binding leader sequence (39) in plasmid pTRGA (Fig. 1A). The *trp* promoter has been used for the direct expression in *E. coli* of large quantities of human H-*ras* p21 (37) and many other proteins such as human tumor necrosis factor (46). However, introduction of pTRGA into *E. coli* and derepression of the *trp* promoter with IAA did not result in any apparent synthesis of R-*ras* p23 compared to a pBR322 control, as assayed by Coomassie blue staining after SDS-PAGE (data not shown).

To obtain antibody probes for detecting low levels of R-*ras* expression, we used a synthetic oligopeptide corresponding to the predicted R-*ras* amino acid residues 191-209. This hydrophilic carboxyl-terminal-located R-*ras* amino acid sequence has no sequence similarity to any other known *ras* proteins (26). Rabbits immunized with peptide 191-209 coupled to soybean trypsin inhibitor carrier produced antibodies that reacted with the peptide coupled to bovine serum albumin as assayed by immunoblotting. In an immunoblot assay (Fig. 1B) of extracts from *E. coli* harboring either pBR322 (lane 1) or pTRGA (lane 2), there was specific reactivity of peptide 191-209 antibodies with a protein of the predicted R-*ras* size in *E. coli* transformed with pTRGA. This result shows that R-*ras* p23 is expressed directly in *E. coli*, albeit at a low level. The level of R-*ras* p23 expression we observe in *E. coli* precludes the type of direct biochemical analysis performed on highly expressed H-*ras* p21 from *E. coli* (37).

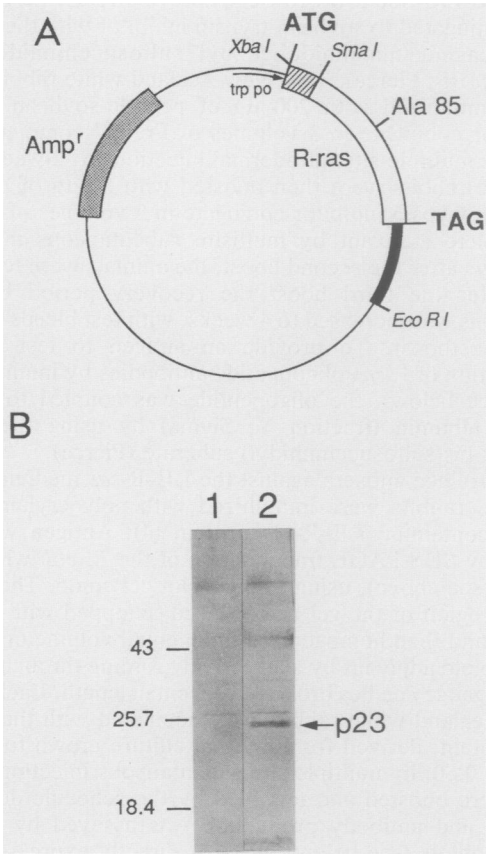


FIG. 1. Direct expression of R-*ras* in *E. coli*. (A) Diagram of the expression vector pTRGA. R-*ras* coding sequences are under the transcriptional control of the *E. coli* tryptophan promoter and operator sequences (trp po). Synthetic linker DNA (see Materials and Methods) is indicated by the hatched region from *Xba*I to *Sma*I immediately 3′ of the *trp* sequences. The translation initiation codon (ATG), 8 bases 3′ of the *Xba*I site, and the translation stop codon (TAG) are indicated at either end of the R-*ras* coding sequence. 3′ untranslated sequences from R-*ras* cDNA are shown by the heavy black bar from the termination codon (TAG) to *Eco*RI. Expression plasmid pTRGT was created by mutation of amino acid Ala 85 to Thr (analogous to the H-*ras* position 59 Ala → Thr mutation) by primer mutagenesis (see Materials and Methods). The β-lactamase gene used to transform *E. coli* harboring pTRGA or pTRGT to ampicillin resistance (Amp$^r$) is indicated by the stippled bar. (B) Immunoblotting of *E. coli* extracts. Whole-cell lysates of IAA-induced *E. coli* harboring pBR322 (lane 1) or pTRGA (lane 2) were fractionated by SDS-PAGE, transferred to nitrocellulose, and probed with R-*ras* oligopeptide 191-209 antiserum. The position of R-*ras* p23 is indicated on the right, with the relative molecular mass (kilodaltons) of size standards shown on the left.

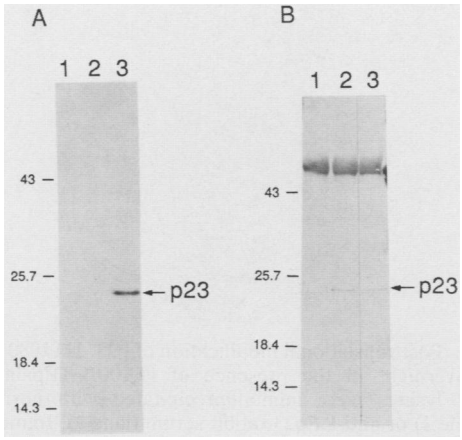


FIG. 2. Autophosphorylation of p23 position 85 Ala → Thr mutant. Whole-cell lysates were prepared from *E. coli* cells harboring pBR322 (lanes 1), pTRGA (lanes 2), or pTRGT (lanes 3), incubated in the presence of [γ-$^{32}$P]GTP and ATP, and then immunoprecipitated with p23 oligopeptide antibodies (see Materials and Methods). Immunoprecipitates were split for duplicate SDS-PAGE runs, and gels were processed for (A) autoradiography of $^{32}$P-labeled proteins or (B) immunoblot analysis of immunoprecipitates for detection of both unlabeled and $^{32}$P-labeled p23.

**Autophosphorylation of mutant R-*ras*.** Phosphorylation of both viral H-*ras* and K-*ras* p21 proteins at threonine 59 (54) in a GTP-dependent manner suggested an indirect assay for the predicted R-*ras* guanosine-specific nucleotide binding. To obtain R-*ras* protein with a phosphoryl acceptor, we engineered a threonine substitution at position 85 of p23, analogous to a p21 position 59 alanine-to-threonine mutation. Phosphorylation of the threonine-substituted R-*ras* protein was detected by immunoprecipitation of *E. coli* extracts after incubation in the presence of [γ-$^{32}$P]GTP and a 30-fold molar excess of ATP (Fig. 2A). Cells carrying pBR322 (Fig. 2, lane 1) or pTRGA (lane 2) did not have any $^{32}$P-labeled proteins precipitated with the peptide 191-209 antibodies. In cells harboring pTRGT, the R-*ras* threonine-substitution mutant, there was specific $^{32}$P labeling of R-*ras* (lane 3). The presence of R-*ras* p23 refractory to labeling by [γ-$^{32}$P]GTP in the extract from cells harboring pTRGA was assayed by probing Western blots (immunoblots) of the in vitro kinase reaction immunoprecipitates (Fig. 2B). R-*ras* p23 was absent from the pBR322 *E. coli* lysate (lane 1) and present in both the pTRGA (lane 2) and pTRGT (lane 3) *E. coli* lysates. This demonstrates the dependence of phosphorylation on the threonine substitution and shows that immunoprecipitation of R-*ras* p23 by peptide 191-209 antibodies is not influenced either by the conditions of the kinase reaction or by the position 85 threonine substitution. When assayed as described for Fig. 2, the autophosphorylation of threonine-substituted p23 by [γ-$^{32}$P]GTP was not affected by excess CTP or UTP, but could be effectively reduced with unlabeled GTP (data not shown). These data on the threonine 85-dependent phosphorylation of mutant p23 by [γ-$^{32}$P]GTP suggest that R-*ras* p23 has intrinsic guanosine-specific triphosphatase activity.

Immunoprecipitation of R-*ras* p23 from nonionic detergent lysates of *E. coli* resulted in two protein bands (Fig. 2A, lane 3). The upper of these two bands corresponds to the size of p23 detected in *E. coli* ionic detergent lysates (Fig. 1B), with the more prominent lower band approximately 1,000 daltons smaller. We believe this predominant smaller species is a degradation product of R-*ras* p23, possibly resulting from a trypsinlike cleavage near the C-terminally located residues 207-209, Arg-Lys-Lys. Given the independence of the H-*ras* p21 catalytic domain from the C-terminal portion of the molecule (72), one might still expect to observe the enzymatic activity of the smaller R-*ras* p23 species (Fig. 2). The apparent sensitivity of R-*ras* p23 to degradation in nonionic detergent lysates of *E. coli* has hampered our efforts to purify the intact p23 molecule under nondenaturing conditions.

**Identification of human R-*ras* protein.** When peptide 191-209 antibodies were tested against the human fibrosarcoma cell line HT1080, which contains R-*ras* mRNA (33), by both immunoblotting (65) and standard immunoprecipitation procedures (15, 52), no specific reactivity was seen with a protein in the predicted 23,000-dalton molecular mass range. Possible explanations might be that the low level of R-*ras* expression in HT1080 cells (33) made it difficult to detect R-*ras* above background proteins in immunoprecipitates, or that the C-terminal region sequence (amino acids 191 to 209) used as the immunogen was inaccessible to antibodies in mammalian cell detergent lysates. To circumvent these possible difficulties, we produced different antibodies by synthesizing high levels of an R-*ras* fusion protein in *E. coli* and used this fusion protein to immunize rabbits against the entire R-*ras* polypeptide sequence. The sequence encoding R-*ras* was linked to a medium-length leader sequence encoding 101 amino acids from a deletion of the *trp* leader-*trpE* fusion Δ*trpLE1413* (39) (see Materials and Meth-

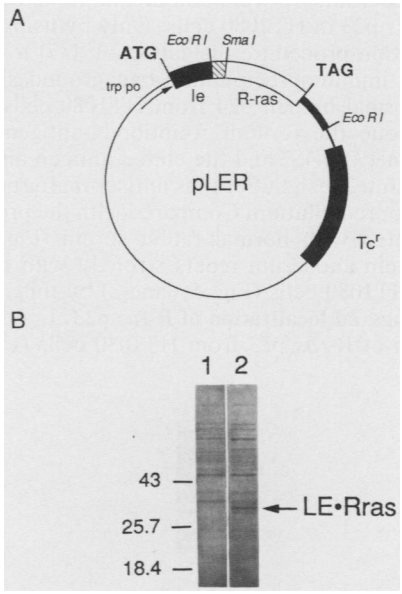


FIG. 3. LE-p23 fusion protein expression in *E. coli*. (A) Diagram of expression vector pLER. Following the tryptophan promoter and operator (trp po), sequences encoding 101 amino acids of the tryptophan medium fusion polypeptide are indicated by a bar beginning at the translation initiation codon (ATG). A hatched box shows the segment of synthetic DNA from *Eco*RI to *Sma*I used to generate an in-frame fusion of LE and R-*ras* coding sequence, with the remaining R-*ras* sequence shown by an open bar ending at the translation termination codon (TAG). The gene conferring resistance to tetracycline (Tc$^r$) is indicated following the fusion protein gene. (B) Synthesis of LE-p23. *E. coli* cells harboring pBR322 (lane 1) or pLER (lane 2) were induced with IAA, and whole-cell extracts were prepared from equal numbers of cells, fractionated by SDS-PAGE, and stained with Coomassie blue.

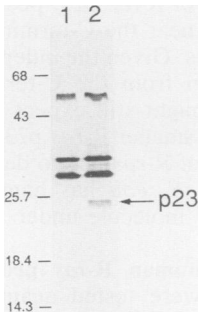


FIG. 4. Detection of directly expressed R-*ras* p23 with LE-p23 antiserum. Rabbit antiserum to the LE-p23 fusion protein was assayed for reactivity to p23 directly expressed in *E. coli* by probing an immunoblot of lysates from IAA-induced *E. coli* harboring pBR322 (lane 1) or pTRGA (lane 2).

ods). The resulting LE-p23 fusion protein expression vector, pLER (Fig. 3A), directed the synthesis of sufficient amounts of LE-p23 (Fig. 3B) for use as an immunogen in rabbits. The presence of the 101-amino-acid LE-leader peptide on the R-*ras* p23 protein significantly increased the steady-state level of protein synthesized compared to directly expressed R-*ras*.

Antiserum from a rabbit immunized with the LE-p23 fusion protein was highly reactive to the p23 directly expressed in *E. coli* (Fig. 4). Using either immunoblotting (65) or immunoprecipitation techniques (15, 52) with the fusion-protein antiserum, we were still unable to detect the endogenous R-*ras* p23 in HT1080 cells. Only by using the elution-reprecipitation procedure of Platt et al. (47) to significantly reduce the immunoprecipitation background signal did we observe normal human p24 from HT1080 cells (Fig. 5). In this technique the protein A-antibody-antigen complex is disrupted in 1% SDS, and the eluted antigen and antibodies are diluted into fresh buffer plus antiserum for a repetition of the immunoprecipitation. Compared with the proteins immunoprecipitated with normal rabbit serum (Fig. 5, lane 1), fusion-protein antiserum reacts strongly with human R-*ras* p23 from HT1080 cells (Fig. 5, lane 2) by this procedure.

**Processing and localization of R-*ras* p23.** In contrast to the single form of R-*ras* p23 from HT1080 cells (Fig. 5), H-*ras*

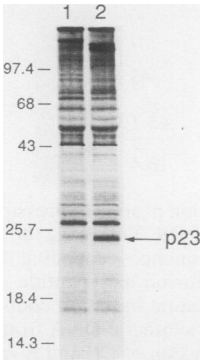


FIG. 5. Immunoprecipitation of human p23. Human fibrosarcoma cell line HT1080 was labeled with L-[$^{35}$S]methionine and L-[$^{35}$S]cysteine and immunoprecipitated with normal rabbit serum (lane 1) or anti–LE-p23 rabbit serum (lane 2). Immunoprecipitates were analyzed by SDS-PAGE and fluorography. The position of human R-*ras* p23 is indicated on the right, and molecular mass standards (kilodaltons) are shown on the left.

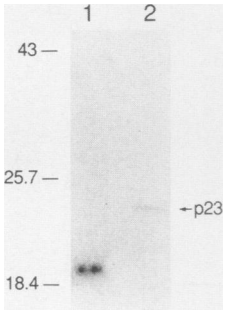


FIG. 6. Posttranslational modification of p23. HT1080 cells were labeled overnight in the presence of [9,10(*n*)-$^{3}$H]palmitic acid. Detergent lysates were immunoprecipitated with normal rabbit serum (lane 1) or anti-LEp23 rabbit serum (lane 2). Immunoprecipitates were analyzed by SDS-PAGE and fluorography. The position of $^{3}$H-labeled p23 is indicated on the right, and protein standards (kilodaltons) are on the left.

p21 is usually detected as a doublet species, with the upper band corresponding to pro-p21 and the lower band corresponding to mature p21 (56). Pulse-chase experiments show that concomitant with the change from pro-p21 to p21 is the addition of palmitic acid to cysteine 186 and localization to the plasma membrane (8, 72, 73). We investigated the processing of R-*ras* p23 by labeling HT1080 cells with [9,10(*n*)-$^{3}$H]palmitic acid and immunoprecipitating with the fusion protein antiserum (Fig. 6). This experiment identifies a $^{3}$H-labeled form of p23 (lane 2) with the same mobility as the L-[$^{35}$S]methionine- and L-[$^{35}$S]cysteine-labeled p23 shown in Fig. 5. Unlike the readily discernible precursor of *ras* p21s, the mobility difference between pro-p23 and p23 in SDS-PAGE may not be easily resolved. Alternatively, the rate of posttranslational modification may be greater for p23 than p21, preventing the detection of pro-p23.

The detection of $^{3}$H-p23 from [9,10(*n*)-$^{3}$H]palmitate-labeled HT1080 cells suggests that R-*ras* p23 is modified by palmitic acid addition. This result leads to the prediction that the mature form of p23 will be membrane associated. To determine the subcellular localization of p23, HT1080 cells were labeled with L-[$^{35}$S]methionine and L-[$^{35}$S]cysteine for 4 h, lysed in hypotonic buffer with a Dounce homogenizer, and separated into S100 crude cytoplasmic and P100 crude membrane fractions by centrifugation at 100,000 × *g*. Immunoprecipitation of S100 and P100 subcellular fractions with normal rabbit serum and fusion protein antiserum (Fig. 7) revealed R-*ras* p23 to be exclusively associated with the P100 membrane fraction (Fig. 7, lane 2B).

**Vector constructions for mammalian expression of normal and mutant R-*ras* proteins.** A human R-*ras* minigene was designed to facilitate in vitro manipulations for R-*ras* expression vector construction. The first four coding exons of R-*ras*, spanning approximately 3.4 kilobases of genomic DNA, were replaced with 453 bp of contiguous coding sequence from cloned R-*ras* cDNA. Expression of this R-*ras* minigene was placed under the control of the SV40 early region promoter (SVE). The resulting expression plasmid, pSVE.RG (Fig. 8), was expected to direct the synthesis of R-*ras* p23 in mammalian cells.

We anticipated that if R-*ras* p23 and H-*ras* p21 have comparable biological properties, this would be revealed by a similar effect of mutant R-*ras* p23 and oncogenic H-*ras* p21 genes on the in vitro transformation of rodent fibroblasts. A substitution analogous to the position 12 glycine-to-valine

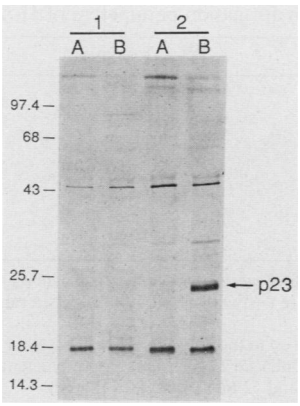


FIG. 7. Subcellular localization of p23. HT1080 cells labeled with L-[$^{35}$S]methionine and L-[$^{35}$S]cysteine were fractionated into S100 cytosol (lanes 1) and P100 membrane (lanes 2) fractions by centrifuging hypotonic lysates at 100,000 × *g* (see Materials and Methods). Subcellular fractions were immunoprecipitated with normal rabbit serum (lanes A) or anti-LE-p23 rabbit serum (lanes B). Samples were analyzed by SDS-PAGE and fluorography. $^{35}$S-labeled p23 is indicated on the right, and molecular mass standards (kilodaltons) are shown on the left.

*ras* p21 transforming mutation was constructed in the R-*ras* minigene by mutagenesis of R-*ras* codon 38 glycine to valine. The expression vector construction for this valine-substituted p23 gene, pSVE.RV, was identical to that used to express the normal R-*ras* p23 allele (Fig. 8, SVE.RG).

Alignment of the R-*ras* p23 218-amino-acid sequence with the 189-residue H-*ras* p21 sequence for optimal homology revealed that R-*ras* p23 has an additional 26 N-terminal amino acids relative to p21 (33). To determine whether this amino-terminal sequence had any detectable effect on the properties of R-*ras* p23, we engineered a deletion mutant of R-*ras* (Fig. 8, SVE.RGΔ1-26). A new translation initiation codon (Fig. 8, ATG*) was created by mutation of R-*ras* codon 27 serine to methionine. This mutation makes the R-*ras* p23 (Δl-26) deletion mutant and H-*ras* p21 translation start sites coincident. The natural R-*ras* p23 translation start site was removed by joining to the SVE promoter at a *Sma*I site 15 bp upstream of the position 27 methionine substitution (Fig. 8). Expression of this R-*ras* p23 (Δ1-26) deletion mutant should result in a 192-amino-acid protein colinear with the H-*ras* p21 for 122 amino acids. There is a single amino acid insertion in the R-*ras* sequence between H-*ras* residues 122 and 123 and a two-residue insertion in the R-*ras* sequence between H-*ras* carboxyl-terminal region residues 181 and 182 (33). These insertion mutations between R-*ras* p23 and H-*ras* p21 lie within two regions of sequence divergence among the H-, K-, and N-*ras* p21s, residues 121 to 132 and 165 and 181 (55), which are not required for the transformation function of activated p21 (74, 75).

An R-*ras* p21-like molecule was also created in the likeness of the T24 oncogene-encoded p21 by mutating p23 (Δ1-26) codon 12 glycine to valine. The expression vector pSVE.RVΔ1-26 should direct the synthesis of a protein closely resembling the codon 12-activated form of H-*ras* p21.

**Verification of R-*ras* alleles by transient expression.** To confirm the identity of the proteins encoded by the expression vectors pSVE.RG, pSVE.RV, pSVE.RGΔ1-26, and pSVE.RVΔ1-26, we assayed for transient R-*ras* gene expression in transfected COS-7 cells (19). We reasoned that amplification of the SVE-containing plasmids in *trans* by T-antigen would result in easily detectable levels of plasmid-directed R-*ras* expression above any endogenous COS-7 cell R-*ras* p23. Immunoprecipitation of COS-7 cells transfected with the control plasmid pNeoDHFR showed the level of endogenous R-*ras* gene expression (Fig. 9, lane 1). Transient expression from pSVE.RG resulted in the synthesis of large amounts of material comigrating with the endogenous COS-7 R-*ras* p23 (Fig. 9, lane 2). This result further confirms our assignment of the protein encoded by the human R-*ras* gene and demonstrates the effectiveness of the expression vector design. Examination of the autoradiogram from this experiment revealed the highly expressed R-*ras* p23 from pSVE.RG and pSVE.RV to be a closely spaced doublet band (Fig. 9). We interpret this observation to mean we are detecting pro-p23 (upper band) and p23 (lower band). This is supported by the redistribution of $^{35}$S-labeled p23 into the upper band by hydroxylamine treatment before SDS-PAGE

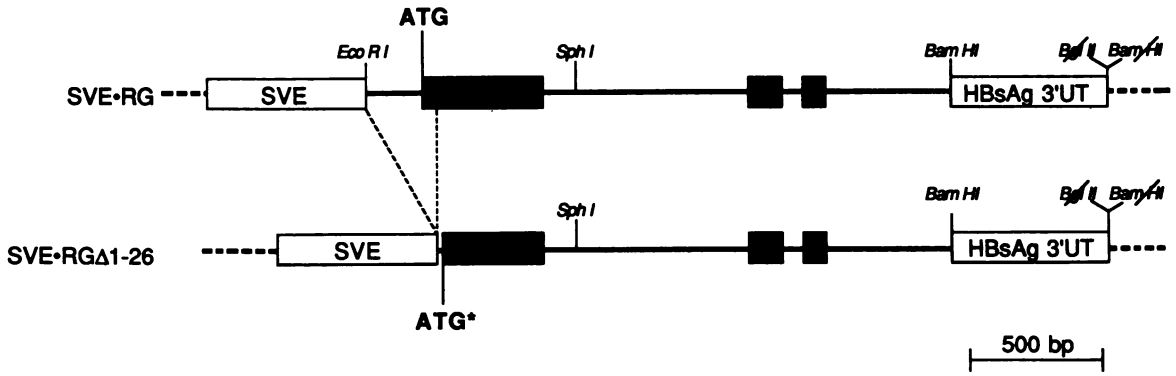


FIG. 8. Expression constructs for normal and mutant R-*ras* alleles. The relevant genetic elements of the R-*ras* expression vectors pSVE.RG and pSVE.RGΔ1-26 are shown, with the coding sequence of the R-*ras* gene indicated by stippled boxes beginning with the translation initiation codon ATG. The three-exon R-*ras* minigene, created by replacing the first four coding exons of the R-*ras* gene with cDNA sequences, is under the transcriptional control of the SV40 early region (SVE), with the hepatitis B surface antigen gene 3′ untranslated region (HBsAg 3′UT) at the 3′ end of the gene to provide an efficient polyadenylation signal. The dashes on either side of the SVE.RG and SVE.RGΔ1-26 constructs indicate the pML-1 vector sequences. The deletion that created the Δ1-26 mutation is indicated by the dashed lines joining the upper (SVE.RG) and lower (SVE.RGΔ1-26) genes. Codon 27 Ser of SVE.RG was mutated to Met (ATG*) to become the new translation initiation codon for SVE.RGΔ1-26. The expression vectors pSVE.RV and pSVE.RVΔ1-26 are the same as their respective normal and amino-terminal deletion mutants, except that Gly (position 38 or 12, respectively) has been mutated to Val, a change analogous to the H-*ras* position 12 Gly → Val transforming mutation.

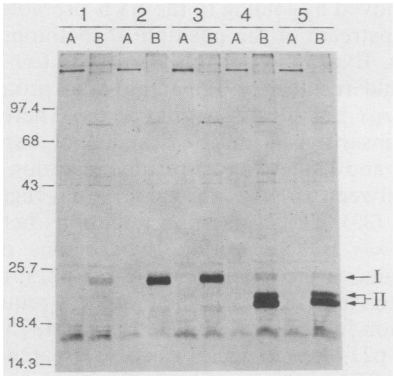


FIG. 9. R-*ras* transient expression. COS-7 cells transfected with (lanes 1) pNeoDHFR, (2) pSVE.RG, (3) pSVE.RV, (4) pSVE.RG Δ1-26, or (5) pSVE.RVΔ1-26 were labeled with L-[$^{35}$S]methionine and L-[$^{35}$S]cysteine before immunoprecipitation with normal rabbit serum (lanes A) or LE–R-ras fusion protein antiserum (lanes B). Immunoprecipitates were analyzed by SDS-PAGE and fluorography. To the right, the position of endogenous COS-7 cell R-*ras* and expression plasmid R-*ras* is indicated by I, and two forms of R-*ras* detected in cells expressing the Δ1-26 mutations are indicated by II. The relative molecular masses (kilodaltons) of size-standard proteins (Bio-Rad) are indicated on the left.

(data not shown). We confirmed the posttranslational modification of R-*ras* p23 expressed from pSVE.RG by immunoprecipitation of $^{3}$H-labeled p23 from transfected COS-7 cells incubated with [9,10(*n*)-$^{3}$H]palmitic acid. Densitometer scanning of an autoradiogram showed the $^{3}$H label on p23 (Fig. 10, lane 2) to be bound in a hydroxylamine-sensitive manner (Fig. 10, lane 3), suggesting that palmitate is covalently attached to p23 via a thioester bond (36, 45).

Transfection of COS-7 cells with the SVE.RV allele resulted in the production of a protein with a slightly retarded mobility (Fig. 9, lane 3) compared with the normal R-*ras* allele (Fig. 9, lane 2). This result directly parallels the altered electrophoretic mobility on SDS-PAGE of *ras* p21 proteins with single-amino-acid substitutions (11, 63) and further underscores the catalytic-domain structural similarities between R-*ras* p23 and *ras* p21 proteins.

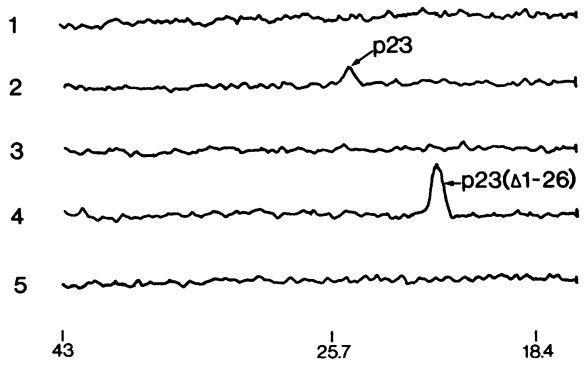


FIG. 10. Palmitate labeling of R-*ras* proteins. COS-7 cells were transfected with (1) pNeoDHFR, (2 and 3) pSVE.RG, (4 and 5) pSVE.RGΔ1-26, labeled with [9,10(*n*)-$^{3}$H]palmitic acid, and immunoprecipitated with R-*ras* fusion protein antiserum. Immunoprecipitates from lines 3 and 5 were treated with 1 M $H_2NOH$-HCl before SDS-PAGE and fluorography. Lanes were scanned with a laser densitometer to illustrate the presence of $^{3}$H-p23 (line 2) and $^{3}$H-p23 (Δ1-26) (line 4). Molecular mass standards (kilodaltons) are shown across the bottom.

TABLE 1. Transformation parameters of H-*ras* R-*ras* alleles

| Plasmid | Focus formation[a] | Agar growth[b] |
|---|---|---|
| pSVEPBL116[c] | − | − |
| pSVET24[c] | + | + |
| pSVE.RG | − | − |
| pSVE.RV | − | − |
| pSVE.RGΔ1-26 | − | − |
| pSVE.RVΔ1-26 | − | − |
| pNeoDHFR | − | − |

[a] No transformed foci were observed with plasmids that scored negative (−). The positive score (+) with pSVET24 reflects a range of 400 to 600 foci per transfection.

[b] A negative score (−) in the soft-agar growth assay is zero viable colonies. Cells transformed by pSVET24 (+) plated with efficiencies from 3 to 5%.

[c] See references 5 and 52 and references therein.

Expression of the amino-terminal truncation mutants SVE.RGΔ1–26 (Fig. 9, lane 4) and SVE.RVΔ1-26 (Fig. 9, lane 5) revealed a slightly reduced mobility for the position 12 valine substitution mutant and the production of two prominent bands with an apparent molecular size difference of approximately 1,000 daltons. The predicted relative molecular mass of the p23 (Δ1-23) mutant is 21,200 daltons, corresponding to the mobility of the lower of the two bands seen in Fig. 9 (lanes 4 and 5). The size difference between the two bands observed with the p23 (Δ1-26) mutants and the heavier distribution of labeled protein into the lower of these bands is similar to the relationship between H-*ras* pro-p21 and mature p21 on SDS-PAGE (56). The correct processing of the R-*ras* p23 (Δ1-26) mutant is shown by labeling of the faster migrating p23 (Δ1-26) species with [9,10(*n*)-$^{3}$H]palmitate in a hydroxylamine-sensitive manner (Fig. 3, lanes 4 and 5).

**Transformation parameters of transfected rat fibroblasts.** Normal and mutant *ras* p21 proteins display context-dependent biological properties that strongly indicate a role for p21s in plasma membrane signal transduction. We used the dominant phenotype of mutant *ras* p21 alleles in malignant transformation as a comparative assay for the biological activity of mutant H-*ras* p21 and R-*ras* p23 alleles (Table 1). Transfection of Rat-1 fibroblasts with the normal H-*ras* p21 expression vector pSVEPBL116 (5) did not result in transformed foci. When Rat-1 cells were transfected with pSVET24, expressing the position 12 valine-substituted p21 of the T24 oncogene (5), we observed the formation of transformed foci overgrowing a stationary monolayer of Rat-1 cells (Table 1). Although the expression of normal R-*ras* p23 from pSVE.RG did not result in the formation of foci, we were surprised to observe no dominant phenotype from any of the mutant R-*ras* alleles carried in plasmids pSVE.RV, pSVE.RGΔ1-26, pSVE.RVΔ1-26 (Table 1). To extend these observations, we cotransfected Rat-1 fibroblasts with pNeoDHFR to allow selection for transfected cells with the antibiotic G418. Even in the presence of this initial selection, all of the R-*ras* alleles failed to transform when pooled clones were maintained in monolayer or were tested for their ability to induce the property of soft-agar growth. The genes carried in pSVEPBL116 and pSVET24 behaved as expected in this assay, with a positive score by pSVET24 in inducing soft-agar growth of transfected Rat-1 fibroblasts (Table 1).

To address the potential problem of a low expression level from the SVE promoter in transfected Rat-1 fibroblasts, we constructed an additional set of vectors utilizing the strong promoter activity of the Rous sarcoma virus long terminal repeat (21). This set of vectors was essentially the same as

those utilizing the SVE promoter (Fig. 8), with the viral long terminal repeat in place of SVE. As with the SVE expression vectors, transfection of Rat-1 fibroblasts with pRSV.RG, pRSV.RV, pRSV.RGΔ1-26, and pRSV.RVΔ1-26 did not induce focus formation or the ability to grow in soft agar. We isolated Rat-1 clones expressing the pRSV.RGΔ1-26 or pRSV.RVΔ1-26 vectors, as assayed by immunoprecipitation, but these cell lines did not display any predilection towards focus formation or growth in soft agar (data not shown).

## DISCUSSION

To elucidate the biochemical and biological properties of proteins encoded by the H-, K-, and N-*ras* family of proto-oncogenes, many groups have undertaken to express the encoded p21 molecule in *E. coli* (24, 26, 31, 37, 41, 60, 66). These efforts have provided sufficient quantities of *ras* p21 to define extensively its intrinsic GTP-binding and GTPase activities (17, 37, 41, 62, 66). We describe here the construction of *E. coli* expression vectors encoding normal and threonine-substituted R-*ras* p23. For cloning of human R-*ras* cDNA into the *E. coli* expression vector we used a synthetic oligonucleotide spanning the first 21 codons of R-*ras*. The GC-rich R-*ras* codons in this region were replaced with commonly used *E. coli* codons (23), and an *Xba*I site immediately 5′ of the translation initiation codon allowed placing of the R-*ras* linker cDNA sequence under the direct control of *trp* promoter and ribosome binding leader sequences (39). Although this strategy has been successfully exploited in the past for high-level direct expression of many foreign proteins in *E. coli* (24, 46), it was only by using antibodies to an oligopeptide antigen that we were able to detect a low level of R-*ras* p23 expression in immunoblots of fractionated *E. coli* extracts. High steady-state levels of p23 expression were achieved by the addition of 101 amino-terminal residues in the LE-p23 fusion protein, with a resulting increase in the *E. coli* doubling time by approximately 16-fold. This result suggested to us that the R-*ras* p23 polypeptide might be inherently toxic to *E. coli*.

To test indirectly for the predicted guanosine-specific nucleotide binding of R-*ras* p23, we chose to expose a cryptic phosphoryl-acceptor site by creating a position 85 alanine-to-threonine substitution. This is analogous to a p21 position 59 threonine substitution, which results in autophosphorylation in a GTP-dependent manner (54). The threonine substitution-specific phosphorylation R-*ras* p23 in the presence of [$\gamma$-$^{32}$P]GTP demonstrates the biochemical similarity of R-*ras* p23 and the *ras* p21s. Variability in the amount of p23 immunoprecipitated from different in vitro kinase reactions has hampered quantitation of the effect of competing unlabeled nucleotides on the autophosphorylation of threonine-substituted p23 with [$\gamma$-$^{32}$P]GTP. However, we could qualitatively normalize for the amount of p23 immunoprecipitated by probing Western blots of immunoprecipitates, as described for Fig. 2. In this way we observed the specific reduction in threonine-substituted p23 labeling by excess unlabeled GTP. Direct proof of autophosphorylation of threonine 85-substituted R-*ras* in *E. coli* lysates would require a demonstration of zero-order kinetics for phosphorylation. In the absence of such data, it is possible that the threonine 85 substitution has provided a substrate for an *E. coli* kinase. We consider this interpretation to be unlikely, given the specificity of procaryotic kinases for bacterial substrates and their requirement for ATP as a phosphoryl donor (16, 68, 69). We therefore interpret our findings as supporting the supposition, based on a high degree of sequence identity (33), that the p23 guanosine-specific nucleotide-binding site has a structure comparable to that of the *ras* p21 proteins and other members of the GTP-binding protein superfamily (25, 28, 30, 32).

To further outline the biochemical similarities of R-*ras* p23 and p21s, we characterized the expression of p23 in the human fibrosarcoma cell line HT1080. The identification of human p23 with fusion-protein antibodies that react with p23 directly expressed in *E. coli* confirms our assignment of the R-*ras* gene coding region (33). The specific $^{3}$H labeling of p23 in the presence of [9,10(*n*)-$^{3}$H]palmitic acid strongly implies that p23 is posttranslationally modified by palmitation of cysteine 215. Although we have not proved the exact chemical form of the $^{3}$H label on p23, or its location on the molecule, our interpretation is consistent with the presence of the consensus carboxyl-terminal palmitation sequence Cys-A-A-X, where A is an aliphatic amino acid and X is the C-terminal amino acid (33). In H-*ras* p21 the cysteine residue of this C-terminal sequence is acylated, presumably through a thio-ester bond (8, 72, 73). Since the C-terminal cysteine of this C-terminal sequence is required for membrane localization and transformation by *ras* p21 (72, 73), it is assumed that acylation with palmitate is a necessary event for *ras* protein subcellular localization. The specific association of R-*ras* p23 with the P100 membrane fraction from HT1080 cells is consistent with the localization predicted from the C-terminal consensus acylation sequence.

The data we present here on the *E. coli* expression of R-*ras* p23 and the analysis of normal p23 expression in human HT1080 cells are consistent with the predictions from primary sequence comparisons of R-*ras* with its most closely related homologs, the p21 proto-oncogene products (33). These data on the properties of R-*ras* p23 strengthen the inference that the *ral* (7) and more distantly related *rho* (35) gene products will also encode membrane-associated GTPases.

The apparently correct biosynthesis and posttranslational modification of the normal and mutant R-*ras* proteins from pSVE.RG, pSVE.RV, pSVE.RGΔ1-26, and pSVE.RV Δ1-26 strongly indicated that these proteins would be found in the context of their normal biological function. Transfection of these R-*ras* p23 allele expression vectors into rat fibroblasts provided a comparative assay with H-*ras* p21 alleles for biological activity. Neither the position 38 valine-substituted R-*ras* p23 nor the position 12 valine-substituted R-*ras* p21-like proteins resulted in focus formation in monolayer or anchorage-independent growth of transfected Rat-1 cells. Substitution of the SV40 early region promoter with the Rous sarcoma virus long terminal repeat did not alter our findings. In addition, Rat-1 cell lines expressing pRSV-RGΔ1-26 and pRSV.RGΔ1-26, as determined by immunoprecipitation, did not display a transformed phenotype (data not shown). Although we cannot rule out species specificity, having transfected rodent cells with a human gene, we do not consider this a likely explanation for the lack of an R-*ras* transforming function. We may also rule out the possibility that R-*ras* proteins are entirely out of context in rat fibroblasts and serve no normal function there. By immunoprecipitation we have found that the R-*ras* protein is present in Rat-1 cells (data not shown) at a level similar to that in human HT1080 cells. We interpret our data as indicating that rat fibroblasts are not sensitive to neoplastic transformation by mutant R-*ras* alleles due to specific biological properties of R-*ras* p23.

The biochemical similarities of *ras* proteins to the adenylyl cyclase G-proteins (18) and the effect of mutant p21 molecules on malignant transformation (67) implicate the *ras* p21 gene products as components of a proliferation signal transduction mechanism. The relationship of this activity of *ras* p21s to the normal function of R-*ras*, *ral*, or *rho* gene products remains to be elucidated. In its role as a signal transduction molecule, H-*ras* p21 may function to modulate growth factor-dependent cellular proliferation (40). By the analogy of *ras* proteins with adenylyl cyclase-stimulatory and -inhibitory G proteins (18), R-*ras* p23 could function in an opposite manner to H-*ras* p21 in growth factor signal transduction. This type of function for p23 would preclude the identification of R-*ras* transforming alleles. Aside from an R-*ras* p23 function related in apposition in *ras* p21s, one might consider a completely unknown biological role for R-*ras* p23 that is exemplified by the differentiation functions of H-*ras* p21 (2, 3, 43). The expression of *ras* proteins in *Drosophila* brain and ganglia (53) and in *Aplysia* neurons and human nerve tissue (61) implicates these proteins in signal transduction in nonreplicating differentiated cells. We envisage that R-*ras* p23 could play a role in transduction of external stimuli in differentiated cells such as neurons, but we cannot rule out a context-dependent role in the proliferation of some cell types.

## ACKNOWLEDGMENTS

We thank the Genentech DNA Synthesis Group for providing oligonucleotides, John Burnier for providing the R-*ras* oligopeptide, Rik Derynck for providing *E. coli* expression vectors, Tim Bringman for advice on immunocytochemistry, Dan Capon for advice during the early stages of this work, Marty Simonetti for densitometer scans, Jeanne Arch and Charles Galvin, Jr., for preparing the manuscript, and Carol Morita and Kerrie Andow for illustrations.

## LITERATURE CITED

1. **Backman, K., M. Ptashne, and W. Gilbert.** 1976. Construction of plasmids carrying the cI gene of bacteriophage λ. Proc. Natl. Acad. Sci. USA **11**:4174–4178.
2. **Bar-Sagi, D., and J. R. Feramisco.** 1985. Microinjection of the ras oncogene protein into PC12 cells induces morphological differentiation. Cell **42**:841–848.
3. **Birchmeier, C., D. Broek, and M. Wigler.** 1985. Ras proteins can induce meiosis in Xenopus oocytes. Cell **43**:615–621.
4. **Boulard, C., and A. Lecroisey.** 1982. Specific antisera produced by direct immunization with slices of polyacrylamide gel containing small amounts of protein. J. Immunol. Methods **50**:221–226.
5. **Capon, D. J., E. Y. Chen, A. D. Levinson, P. H. Seeburg, and D. V. Goeddel.** 1983. Complete nucleotide sequences of the T24 human bladder carcinoma oncogene and its normal homologue. Nature (London) **302**:33–37.
6. **Capon, D. J., P. H. Seeburg, J. P. McGrath, J. S. Hayflick, U. Edman, A. D. Levinson, and D. V. Goeddel.** 1983. Activation of Ki-*ras2* in human colon and lung carcinoma by two different point mutations. Nature (London) **304**:507–513.
7. **Chardin, P., and A. Tavitian.** 1986. The ral gene: a new ras related gene isolated by the use of a synthetic probe. EMBO J. **5**:2203–2208.
8. **Chen, Z.-Q., L. S. Ulsh, G. DuBois, and T. Y. Shih.** 1985. Posttranslational processing of p21 *ras* proteins involves palmitylation of the C-terminal tetrapeptide containing cysteine-186. J. Virol. **56**:607–612.
9. **Clark, R., G. Wong, N. Arnheim, D. Nitecki, and F. McCormick.** 1985. Antibodies specific for amino acid 12 of the ras oncogene product inhibit GTP binding. Proc. Natl. Acad. Sci. USA **82**:5280–5284.
10. **Crowley, C., C.-C. Liu, and A. D. Levinson.** 1983. Plasmid-directed synthesis of hepatitis B surface antigen in monkey cells. Mol. Cell. Biol. **3**:44–55.
11. **Der, C. J., and G. M. Cooper.** 1983. Altered gene products are associated with activation of cellular ras$^k$ genes in human lung and colon carcinomas. Cell **32**:201–208.
12. **Derynck, R., A. B. Roberts, M. E. Winkler, E. Y. Chen, and D. V. Goeddel.** 1984. Human transforming growth factor-α: percursor structure and expression in *E. coli*. Cell **38**:287–297.
13. **Fiers, W., R. Contreras, G. Haegeman, R. Rogiers, A. Van de Voorde, H. Van Heuverswyn, J. Van Herreweghe, G. Volckaert, and M. Ysebaert.** 1978. Complete nucleotide sequence of SV40 DNA. Nature (London) **273**:113–120.
14. **Frost, E., and J. Williams.** 1978. Mapping temperature sensitive and host-range mutations of adenovirus type 5 by marker rescue. Virology **91**:39–50.
15. **Furth, M. E., L. J. Davis, B. Fleurdelys, and E. M. Scolnick.** 1982. Monoclonal antibodies to the p21 products of the transforming gene of Harvey murine sarcoma virus and of the cellular *ras* gene family. J. Virol. **43**:294–304.
16. **Garnak, M., and H. C. Reeves.** 1979. Purification and properties of phosphorylated isocitrate dehydrogenase of *Escherichia coli*. J. Biol. Chem. **254**:7915–7920.
17. **Gibbs, J. B., I. S. Sigal, M. Poe, and E. M. Scolnick.** 1984. Intrinsic GTPase activity distinguishes normal and oncogenic ras p21 molecules. Proc. Natl. Acad. Sci. USA **81**:5704–5708.
18. **Gilman, A. G.** 1984. G proteins and dual control of adenylate cyclase. Cell **36**:577–579.
19. **Gluzman, Y.** 1981. SV40-transformed simian cells support the replication of early SV40 mutants. Cell **23**:175–182.
20. **Goeddel, D. V., E. Yelverton, A. Ullrich, H. L. Heyneker, G. Miozzari, W. Holmes, P. H. Seeburg, T. Dull, L. May, N. Stebbing, R. Crea, S. Maeda, R. McCandliss, A. Sloma, J. M. Tabor, M. Gross, P. C. Familetti, and S. Pestka.** 1980. Human leukocyte interferon produced by *E. coli* is biologically active. Nature (London) **287**:411–416.
21. **Gorman, C. M., G. T. Merlino, M. C. Willingham, I. Pastan, and B. H. Howard.** 1982. The Rous sarcoma virus long terminal repeat is strong promoter when introduced into a variety of eukaryotic cells by DNA-mediated transfection. Proc. Natl. Acad. Sci. USA **79**:6777–6781.
22. **Graham, F. L., and A. J. van der Eb.** 1973. A new technique for the assay of infectivity of human adenovirus 5 DNA. Virology **52**:456–467.
23. **Grantham, R., C. Gautier, M. Gouy, M. Jacobzone, and R. Mercier.** 1981. Codon catalog usage is a genome strategy modulated for gene expressivity. Nucleic Acids Res. **9**:r43–r74.
24. **Gross, M., R. W. Sweet, G. Sathe, S. Yokoyama, O. Fasano, M. Goldfarb, M. Wigler, and M. Rosenberg.** 1985. Purification and characterization of human H-*ras* proteins expressed in *Escherichia coli*. Mol. Cell. Biol. **5**:1015–1024.
25. **Halliday, K. R.** 1984. Regional homology in GTP-binding proto-oncogene products and elongation factor. J. Cyclic Nucleotide Protein Phosphorylation Res. **9**:435–448.
26. **Hattori, S., L. S. Ulsh, K. Halliday, and T. Y. Shih.** 1985. Biochemical properties of a highly purified v-*ras*$^H$ protein over-produced in *Escherichia coli* and inhibition of its activities by a monoclonal antibody. Mol. Cell. Biol. **5**:1449–1455.
27. **Hughes, S. M.** 1983. Are guanine nucleotide binding proteins a distinct class of regulatory proteins? FEBS Lett. **164**:1–8.
28. **Jurnak, F.** 1985. Structure of the GDP domain of EF-Tu and location of amino acids homologous to ras oncogene protein. Science **230**:32–36.
29. **Laemmli, U. K.** 1977. Cleavage of structural proteins during the assembly of the head of bacteriophage T4. Nature (London) **227**:680–685.
30. **Leberman, R., and U. Egner.** 1984. Homologies in the primary structure of GTP-binding proteins: the nucleotide binding site of EF-Tu and p21. EMBO J. **3**:339–341.
31. **Local, J. C., E. Santos, V. Notario, M. Barbacid, S. Yamazaki, H. F. Kung, C. Seamans, S. McAndrew, and R. Crowl.** 1984. Expression of normal and transforming H-ras genes in *Escherichia coli* and purification of their encoded p21 proteins. Proc. Natl. Acad. Sci. USA **81**:5305–5309.
32. **Lochrie, M. A., J. B. Hurley, and M. I. Simon.** 1985. Sequence

of the alpha subunit of photoreceptor G-protein: homologies between transducin, ras, and elongation factors. Science **228**:96–97.
33. **Lowe, D. G., D. J. Capon, E. Delwart, A. Y. Sakaguchi, S. L. Naylor, and D. V. Goeddel.** 1987. Structure of the human and murine R-ras genes, novel genes closely related to ras proto-oncogenes. Cell **48**:137–146.
34. **Lusky, M., and M. Botchan.** 1981. Inhibition of SV40 replication in simian cells by specific pBR322 DNA sequences. Nature (London) **293**:79–81.
35. **Madaule, P., and R. Axel.** 1985. A novel ras-related gene family. Cell **41**:31–40.
36. **Magee, A. I., and S. A. Courtneidge.** 1985. Two classes of fatty acylated proteins exist in eukaryotic cells. EMBO J. **4**:1137–1144.
37. **McGrath, J. P., D. J. Capon, D. V. Goeddel, and A. D. Levinson.** 1984. Comparative biochemical properties of normal and activated human *ras* p21 protein. Nature (London) **310**:644–649.
38. **McGrath, J. P., D. J. Capon, D. H. Smith, E. Y. Chen, P. H. Seeburg, D. V. Goeddel, and A. D. Levinson.** 1983. Structure and organization of the human Ki-*ras* proto-oncogene and a related processed pseudogene. Nature (London) **304**:501–506.
39. **Miozzari, G. F., and C. Yanofsky.** 1978. Translation of the leader region of the *Escherichia coli* tryptophan operon. J. Bacteriol. **133**:1457–1466.
40. **Mulcahy, L. S., M. R. Smith, and D. W. Stacey.** 1985. Requirement for *ras* proto-oncogene function during serum stimulated growth of NIH 3T3 cells. Nature (London) **313**:241–243.
41. **Nakano, E. T., M. A. Rao, M. Perucho, and M. Inouye.** 1978. Expression of the Kirsten *ras* viral and human proteins in *Escherichia coli*. J. Virol. **61**:302–307.
42. **Napier, M. A., R. L. Vandlen, G. Albers-Schonberg, R. F. Nutt, S. Brady, T. Lyle, R. Winquist E. P. Faison, L. A. Heinel, and E. H. Blaine.** 1984. Specific membrane receptors for atrial natriuretic factor in renal and vascular tissues. Proc. Natl. Acad. Sci. USA **81**:5946–5950.
43. **Noda, M., M. Ko, A. Ogura, D. Liu, T. Amano, T. Takano, and Y. Ikawa.** 1985. Sarcoma viruses carrying *ras* oncogenes induce differentiation-associated properties in a neuronal cell line. Nature (London) **318**:73–75.
44. **Norrander, J., T. Kempe, and J. Messing.** 1983. Construction of improved M13 vectors using oligodeoxynucleotide-directed mutagenesis. Gene **27**:101–106.
45. **Olson, E. N., D. A. Towler, and L. Glasser.** 1985. Specificity of fatty acylation of cellular proteins. J. Biol. Chem. **260**:3784–3790.
46. **Pennica, D., G. E. Nedwin, J. S. Hayflick, P. H. Seeburg, R. Derynck, M. A. Palladino, W. J. Kohr, B. B. Aggarwal, and D. V. Goeddel.** 1984. Human tumor necrosis factor: precursor structure, expression and homology to lymphotoxin. Nature (London) **312**:724–729.
47. **Platt, E. J., K. Karlsen, A. Lopez-Valdivieso, P. W. Cook, and G. L. Firestone.** 1986. Highly sensitive immunoadsorption procedure for detection of low-abundance proteins. Anal. Biochem. **156**:126–135.
48. **Rosenthal, A. R., P. B. Lindquist, T. S. Bringman, D. V. Goeddel, and R. Derynck.** 1986. Expression in rat fibroblasts of a human transforming growth factor-α cDNA results in transformation. Cell **46**:301–309.
49. **Sanger, F., S. Nicklen, and A. Coulson.** 1977. DNA sequencing with chain-terminating inhibitors. Proc. Natl. Acad. Sci. USA **74**:5463–5467.
50. **Saravis, C. A.** 1984. Improved blocking of non-specific antibody binding sites on nitrocellulose membranes. Electrophoresis **5**:54–55.
51. **Scolnick, E. M., A. G. Papageorge, and T. Y. Shih.** 1979. Guanine nucleotide binding activity as an assay for the src protein of rat-derived murine sarcoma viruses. Proc. Natl. Acad. Sci. USA **76**:5355–5359.
52. **Seeburg, P. H., W. W. Colby, D. J. Capon, D. V. Goeddel, and A. D. Levinson.** 1984. Biological properties of human c-Ha-*ras1* genes mutated at codon 12. Nature (London) **312**:71–75.
53. **Segal, D., and B.-Z. Shilo.** 1986. Tissue localization of *Drosophila melanogaster ras* transcripts during development. Mol. Cell. Biol. **6**:2241–2248.
54. **Shih, T. Y., P. E. Stokes, G. W. Smythers, R. Dhar, and S. Oroszlan.** 1982. Characterization of the phosphorylation sites and the surrounding amino acid sequences of the p21 transforming proteins coded for by the Harvey and Kirsten strains of murine sarcoma viruses. J. Biol. Chem. **257**:11767–11773.
55. **Shih, T. Y., and M. O. Weeks.** 1984. Oncogenes and cancer: the p21 ras genes. Cancer Invest. **2**:109–123.
56. **Shih, T. Y., M. O. Weeks, P. Gruss, P. Dhar, S. Oroszlan, and E. Scolnick.** 1982. Identification of a precursor in the biosynthesis of the p21 transforming protein of Harvey murine sarcoma virus. J. Virol. **42**:253–261.
57. **Shimizu, K., D. Birnbaum, M. A. Ruley, O. Fasano, Y. Suard, L. Edlund, E. Taparowsky, M. Goldfarb, and M. Wigler.** 1983. Structure of the Ki-*ras* gene of the human lung carcinoma cell line Calu-1. Nature (London) **304**:497–500.
58. **Simonsen, C. C., and A. D. Levinson.** 1983. Isolation and expression of an altered mouse dihydrofolate reductase cDNA. Proc. Natl. Acad. Sci. USA **80**:2495–2499.
59. **Southern, P. J., and P. Berg.** 1982. Transformation of mammalian cells to antibiotic resistance with a bacterial gene under control of the SV40 early region promoter. J. Mol. Appl. Genet. **1**:327–341.
60. **Stein, R. B., P. S. Robinson, and E. M. Scolnick.** 1984. Photoaffinity labeling with GTP of viral p21 *ras* protein expressed in *Escherichia coli*. J. Virol. **50**:343–351.
61. **Swanson, M. E., A. M. Elste, S. M. Greenberg, J. H. Schwartz, T. H. Aldrich, and M. E. Furth.** 1986. Abundant expression of ras proteins in *Aplysia* neurons. J. Cell Biol. **103**:485–492.
62. **Sweet, R. W., S. Yokoyama, T. Kamata, J. R. Feramisco, M. Rosenberg, and M. Gross.** 1984. The product of *ras* is a GTPase and T24 oncogenic mutant is deficient in this activity. Nature (London) **311**:273–275.
63. **Tabin, C. J., S. M. Bradley, C. I. Bargmann, R. A. Weinberg, A. Papageorge, E. M. Scolnick, R. Dhar, D. R. Lowy, and E. H. Chang.** 1982. Mechanism of activation of a human oncogene. Nature (London) **300**:143–149.
64. **Taparowsky, E., K. Shimizu, M. Goldfarb, and M. Wigler.** 1983. Structure and activation of the human N-ras gene. Cell **34**:581–586.
65. **Towbin, H., T. Staehelin, and J. Gordon.** 1979. Electrophoretic transfer of proteins from polyacrylamide gels to nitrocellulose sheets: procedure and some applications. Proc. Natl. Acad. Sci. USA **76**:4350–4354.
66. **Trahey, M., R. J. Milley, G. E. Cole, M. Innis, H. Paterson, C. J. Marshall, A. Hall, and F. McCormick.** 1987. Biochemical and biological properties of the human N-*ras* p21 protein. Mol. Cell. Biol. **7**:541–544.
67. **Varmus, H. E.** 1984. The molecular genetics of cellular oncogenes. Annu. Rev. Genet. **18**:553–612.
68. **Wang, J. Y. J., and D. E. Koshland.** 1978. Evidence of protein kinase activities in the prokaryote *Salmonella typhimurium*. J. Biol. Chem. **253**:7605–7608.
69. **Wang, J. Y. J., and D. E. Koshland.** 1981. The identification of distinct protein kinases and phosphatases in the prokaryote *Salmonella typhimurium*. J. Biol. Chem. **256**:4640–4648.
70. **Weinberg, R. A.** 1985. The action of oncogenes in the cytoplasm and nucleus. Science **200**:770–776.
71. **Willingham, M. C., I. Pastan, T. Y. Shih, and E. M. Scolnick.** 1980. Localization of the src gene product of the Harvey strain of MSV to the plasma membrane of transformed cells by electron microscopic immunocytochemistry. Cell **19**:1005–1014.
72. **Willumsen, B. M., A. Christensen, N. L. Hubbert, A. G. Papageorge, and D. R. Lowy.** 1984. The p21 *ras* C-terminus is required for transformation and membrane association. Nature (London) **310**:583–586.
73. **Willumsen, B. M., K. Norris, A. G. Papageorge, N. L. Hubbert, and D. R. Lowy.** 1984. Harvey murine sarcoma virus p21 ras protein: biological and biochemical significance of the cysteine nearest the carboxyl terminus. EMBO J. **3**:2581–2585.
74. **Willumsen, B. M., A. G. Papageorge, N. Hubbert, E. Bekesi, H.-F. Kung, and D. R. Lowy.** 1985. The transforming p21 ras

protein: flexibility in the major variable region linking the catalytic and membrane-anchoring domains. EMBO J. **4**:2893–2896.

75. **Willumsen, B. M., A. G. Papageorge, H.-F. Kung, E. Bekesi, T. Robins, M. Johnsen, W. C. Vass, and D. R. Lowy.** 1986. Mutational analysis of a *ras* catalytic domain. Mol. Cell. Biol. **6**:2646–2654.
76. **Yanisch-Peron, C., J. Vieira, and J. Messing.** 1985. Improved M13 phage cloning vectors and host strains: nucleotide sequences of the M13mp18 and pUC19 vectors. Gene **33**:103–119.
77. **Zoller, M., and M. Smith.** 1984. Oligonucleotide-directed mutagenesis: a simple method using two oligonucleotide primers and a single-stranded DNA template. DNA **3**:479–488.